Electronic Supplementary Material (ESI) for Journal of Materials Chemistry A.

Electronic Supplymentary Information

Co-Mo_2N composite on nitrogen-doped carbon matrix with hydrogen evolution activity comparable to Pt/C in alkaline media

Xuewei Lang, [ab] *Muhammad Abdul Qadeer,* [ab] *Guoqiang Shen,* [ab] *Rongrong Zhang,* [ab] *Sichao Yang,* [ab] *Jiayi An,* [ab] *Lun Pan,* [ab] *Ji-Jun Zou*[*ab]

[a] *Key Laboratory for Green Chemical Technology of the Ministry of Education, School of Chemical Engineering and Technology, Tianjin University, Tianjin 300072, China.*

[b] *Collaborative Innovative Center of Chemical Science and Engineering (Tianjin), Tianjin 300072, China.*

* *E-mail: jj_zou@tju.edu.cn*

1. Experimental section

1.1 Materials

Molybdenum trioxide (MoO_3), cobalt chloride hexahydrate ($CoCl_2 \cdot 6H_2O$) and melamine ($C_3N_3(NH_2)_3$) were provided from Aladin Ltd (Shanghai, China). Urea ($CO(NH_2)_2$) was purchased from Tianjin Guangfu Fine Chemical Research Institute. 20wt% Pt/C was supplied by Johnson Matthey. Milli-Q ultrapure water (> 18.25MΩ cm) was used in all experiments.

1.2 Synthesis of Co-Mo_2N@NC

The Co-Mo_2N@NC electrocatalyst was prepared by a two-step process. First, the bimetal hydroxide was synthesized *via* a simple hydrothermal reaction. Typically, $CoCl_2 \cdot 6H_2O$ (1.5 mmol), MoO_3 (1.5 mmol) and urea (3 mmol) were dispersed in 20 mL of deionized under stirring for 0.5 h. Then the dispersion reacted in a Teflon-lined stainless-steel autoclave at 200 °C for 16 h. The HNO_3-treated melamine was synthesized according to previous report[1]. First, the mixture of 1.0 g melamine and 30 mL ethylene glycol was stirred for 20 min to form solution A. 8 mL concentrated HNO_3 (65–68wt%) and 52 mL deionized water were diluted to form solution B. After that, solution A and solution B were mixed followed with 20 min stirring. The obtained HNO_3-treated melamine was washed with deionized water and ethanol several times and dried at 60 °C for 12 h.

1.0 g of HNO_3-treated melamine and 100 mg of bimetal hydroxide were added into 20 mL ethanol, stirring overnight to form an even suspension. After evaporating the ethanol, the mixture was calcined at 550 ℃ for 4 h with the heating rate of 1.0 ℃

min^{-1} in argon atmosphere. HNO_3-treated melamine played the roles of both reductant and N source during calcination to fabricate Co-Mo_2N@NC.

Co_x-Mo_2N@NC with different Co/Mo molar ratio (x=0.5 and 2) was fabricated by the same procedure. Reference sample Co@NC was prepared by hydrothermal reaction of only $CoCl_2 \cdot 6H_2O$ (3 mmol) and urea (3 mmol). Mo_2N@NC was fabricated by heating MoO_3 (100 mg) with HNO_3-treated melamine (1.0 g).

1.3 Catalyst characterization

The morphology of catalysts was characterized by S-4800 field emission scanning electron microscope (FESEM, Hitachi, Japan) and a transmission electron microscope (TEM, JEM-2100F, Japan). X-ray diffraction (XRD) patterns were conducted on a Bruker D8 Focus equipped with nickel-filtered Cu Kα radiation (λ= 1.54056 Å) at a scan rate of 5° min^{-1}. X-ray photoelectron spectroscopy (XPS) measurements were conducted on an ESCALAB250xi electron spectrometer using Al Kα source as radiation source. Element compositions were analyzed by inductively coupled plasma optical emission spectrometer (ICP-OES) measurements which were carried out on a VISTA-MPX EL02115765 instrument. Hydrogen temperature-programmed desorption (H_2-TPD) experiments were performed on Chembet Pulsar (Quantachrome Instruments, USA). 50 mg of sample was pre-treated at 300 °C for 3 h in hydrogen atmosphere and then was cleaned with helium gas flow at 50 °C for 30 min to remove weakly adsorbed H_2. TPD process was performed by heating the sample from 50 °C to 800 °C at a ramp rate of 10 °C min^{-1} under helium atmosphere.

1.4 Electrochemical measurements

All the electrochemical measurements were measured with IVIUMSTAT workstation (Ivium Technologies BV, the Netherlands) in a typical three-electrode system. A graphite rod was used as the counter electrode and a Hg/HgO as the reference electrode. The Hg/HgO reference electrode was calibrated with respect to the reversible hydrogen electrode (RHE) before use. The calibration was conducted in a standard three-electrode system with Hg/HgO as the working electrode, graphite rod as the counter electrode and saturated calomel electrode (SCE) as the reference electrode. All the electrochemical data were converted according to the equation: potential (*vs.* RHE) = $E_{\text{measured},vs.\ \text{Hg/HgO}}$ + 0.059×pH + 0.106 V. 0.106 V was the difference of electrode potential between Hg/HgO electrode and SCE. A glassy carbon electrode with a diameter of 3 mm covered by a thin catalyst film was used as the working electrode. Typically, 5 mg catalyst was dispersed in the mixture of 0.5 mL ethanol and 30 μL Nafion solution. The suspension was sonicated for 2 h to get a homogeneous ink. Then, 10 μL of the ink was dropped onto the surface of the glassy carbon electrode and dried at room temperature. Electrochemical measurements were conducted in 1 M KOH solution. Linear sweep voltammetry (LSV) measurements were first performed for several times until the stable curves were obtained and the scan rate is 5 mV s^{-1}. Electrochemical impedance spectroscopy (EIS) measurements were carried out with frequency ranging from 10^5 Hz to 0.01 Hz under the overpotential at 10 mA cm^{-2}. Electrochemical active surface areas (ECSA) were determined by cyclic voltammetry (CV) at the potential of 0.03−0.13 V, and the scan rates were ranged from 10 mV s^{-1} to 100 mV s^{-1}. The ink of the benchmark 20wt%

Pt/C was prepared in the same way. All data were reported without iR compensation.

2. Catalytic parameter calculations

Electrochemical active surface area (ECSA): ECSA was calculated by following equation[2]:

$$\mathrm{ECSA} = \frac{\mathrm{C_{dl}}}{\mathrm{C_s}}$$

Where C_s was used as 40 μF cm^{-2}, as reported before.[3]

Turnover Frequency Calculations (TOFs): TOF was calculated by following equation:

$$\mathrm{TOF} = \frac{\text{the number of total hydrogen turnovers per cm}^2}{\text{the number of active sites per cm}^2}$$

the number of total hydrogen turnovers per cm^2

$$= \left(j\,\frac{\mathrm{mA}}{\mathrm{cm}^2}\right)\left(\frac{1\ \mathrm{C\ s^{-1}}}{1000\ \mathrm{mA}}\right)\left(\frac{1\ \text{mol of e}^-}{96485.3\ \mathrm{C}}\right)\left(\frac{1\ \text{mol of H}_2}{2\ \text{mol of e}^-}\right)\left(\frac{6.02\times10^{23}\,\mathrm{H_2}\ \text{molecules}}{1\ \text{mol of H}_2}\right)$$

$$= 3.12\times10^{15}\,\frac{\mathrm{H_2/s}}{\mathrm{cm}^2}\times|j|$$

the number of Mo_2N (or Co) active sites per cm^2

= the number of Mo_2N (or Co) active sites per real surface area × ECSA

Mo_2N: $$\left(\frac{6\,\frac{\text{atoms}}{\text{unit cell}}}{72.2\,\frac{\text{Å}^3}{\text{unit cell}}}\right)^{2/3}\times\mathrm{ECSA} = 1.90\times10^{15}\,\frac{\text{atoms}}{\mathrm{cm}^2}\times\mathrm{ECSA}$$

Co: $$\left(\frac{4\,\frac{\text{atoms}}{\text{unit cell}}}{44.52\,\frac{\text{Å}^3}{\text{unit cell}}}\right)^{2/3}\times\mathrm{ECSA} = 2.0\times10^{15}\,\frac{\text{atoms}}{\mathrm{cm}^2}\times\mathrm{ECSA}$$

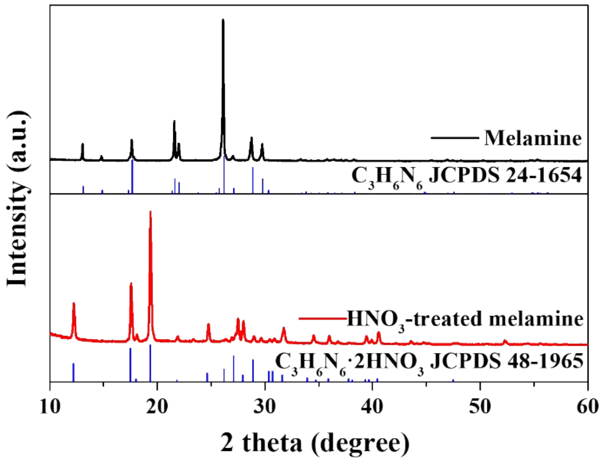

Fig. S1 XRD results of melamine and HNO_3-treated melamine.

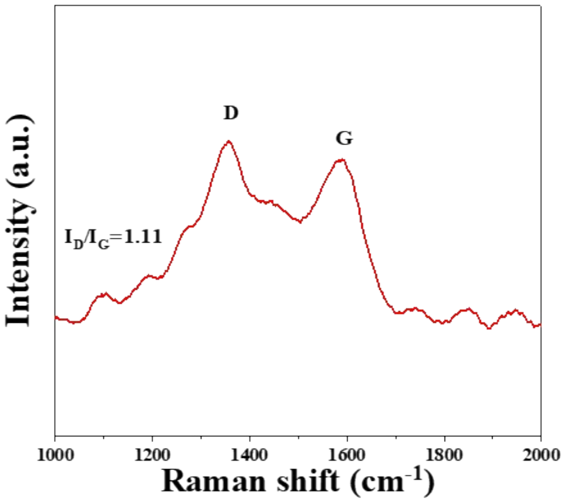

Fig. S2 Raman spectra of Co-Mo_2N@NC.

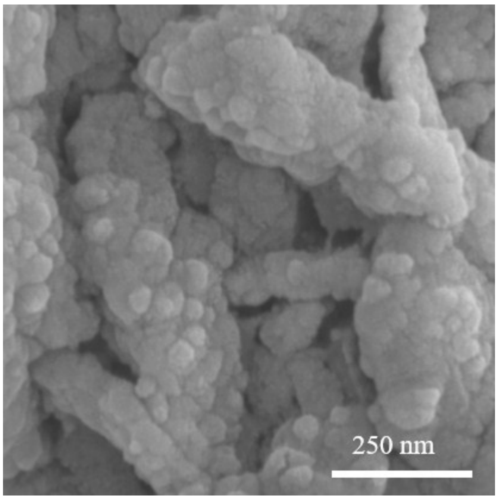

Fig. S3 SEM image Co-Mo_2N@NC.

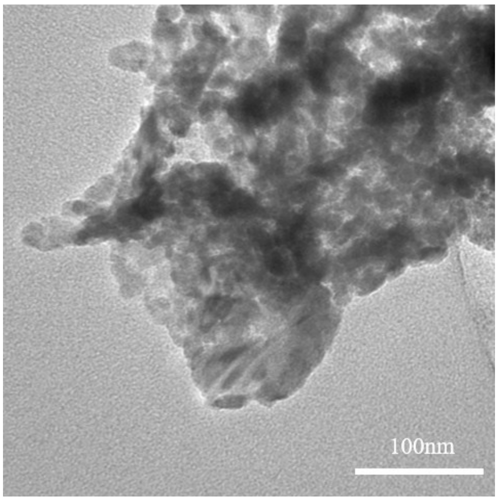

Fig. S4 TEM image of Co-Mo_2N@NC.

Table S1 Elemental compositions of Co-Mo_2N@NC determined by ICP-OES and XPS analysis.

Sample	**ICP (wt%)**			**XPS (wt%)**		
	Co	Mo_2N	N-doped carbon	Co	Mo_2N	N-doped carbon
$Co_{0.5}$-Mo_2N@NC	42.7	24.0	33.3	14.9	48.9	36.2
Co-Mo_2N@NC	42.2	21.4	36.4	18.0	44.3	37.7
Co_2-Mo_2N@NC	42.5	17.2	40.3	26.7	30.8	42.5

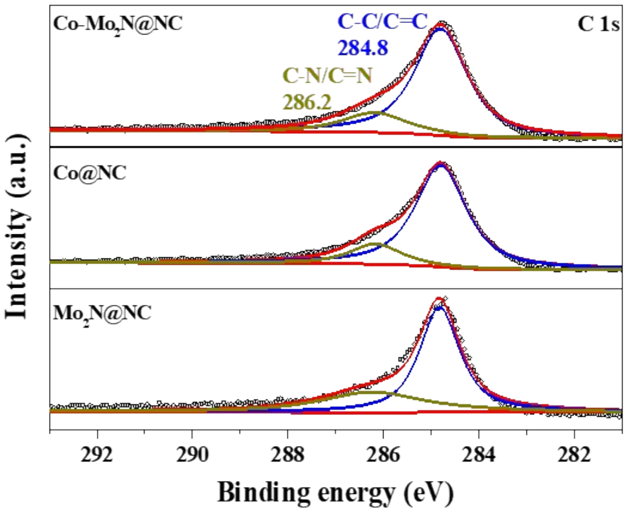

Fig. S5 High-resolution XPS spectra for C 1s of Co-Mo_2N@NC, Co@NC, and Mo_2N@NC.

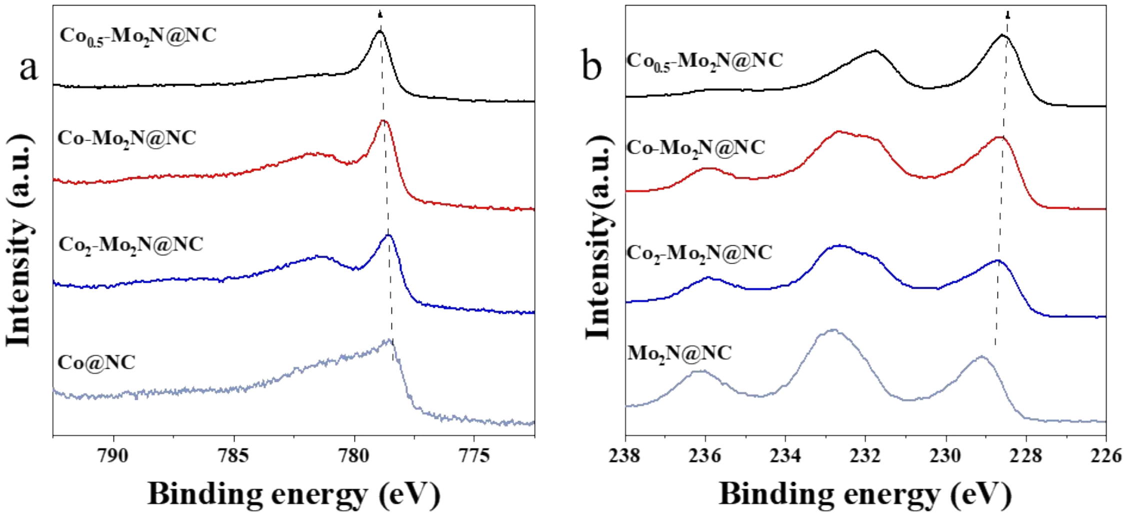

Fig. S6 High-resolution XPS spectra for (a) Co 2p and (b) Mo 3d of Co-Mo_2N@NC with different Co/Mo molar ratio, Co@NC and Mo_2N@NC.

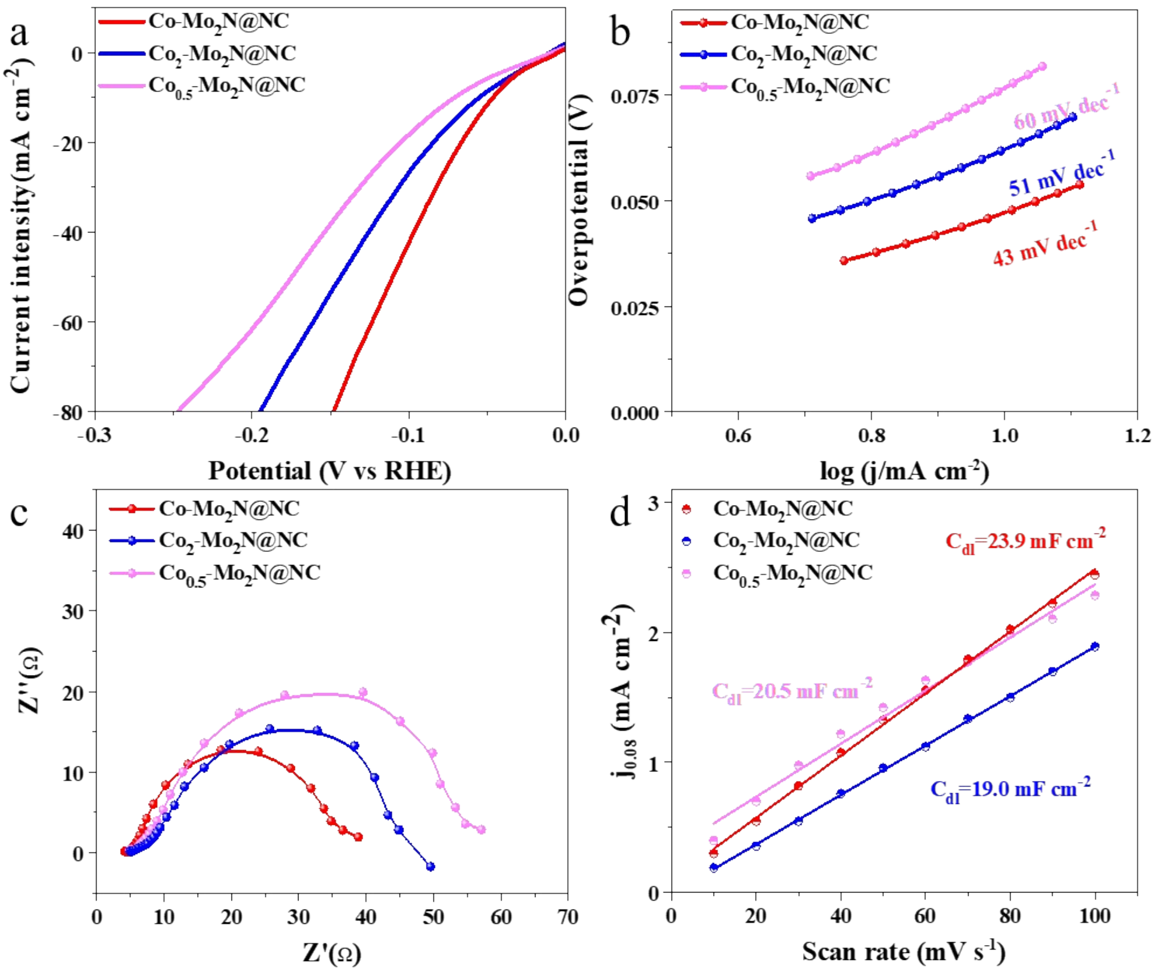

Fig. S7 (a) Polarization curves, (b) Tafel plots, (c) Nyquist plots and (d) C_{dl} obtained at 0.08 V *vs.* RHE of Co-Mo_2N@NC with different Co/Mo molar ratio.

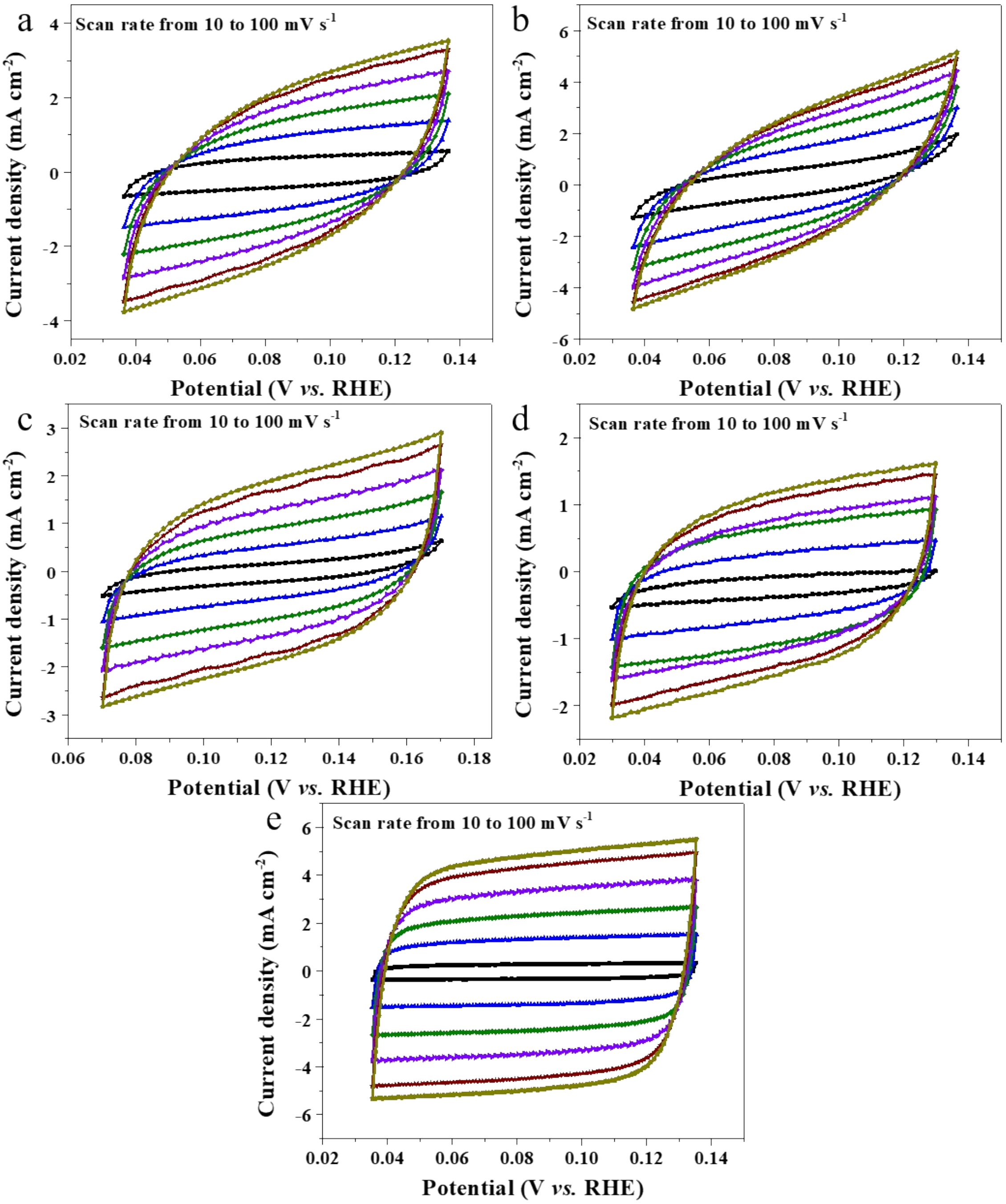

Fig. S8 CV curves of (a-c) Co-Mo_2N@NC with different Co/Mo molar ratio of 0.5, 1 and 2, (d) Co@NC, and (e) Mo_2N@NC.

Table S2 TOFs of Co-Mo_2N@NC, Mo_2N@NC and Co@NC at $\eta = 100$ mV.

Electrocatalyst	η_{10} (mV)	Tafel slope (mV dec^{-1})	C_{dl} (mF cm^{-2})	ESCA (cm^{-2})	TOFs (s^{-1})
Co-Mo_2N@NC	47	43	23.9	597.5	0.1116
Mo_2N@NC	85	54	49.8	1245	0.0207
Co@NC	256	120	12.6	315	0.0054

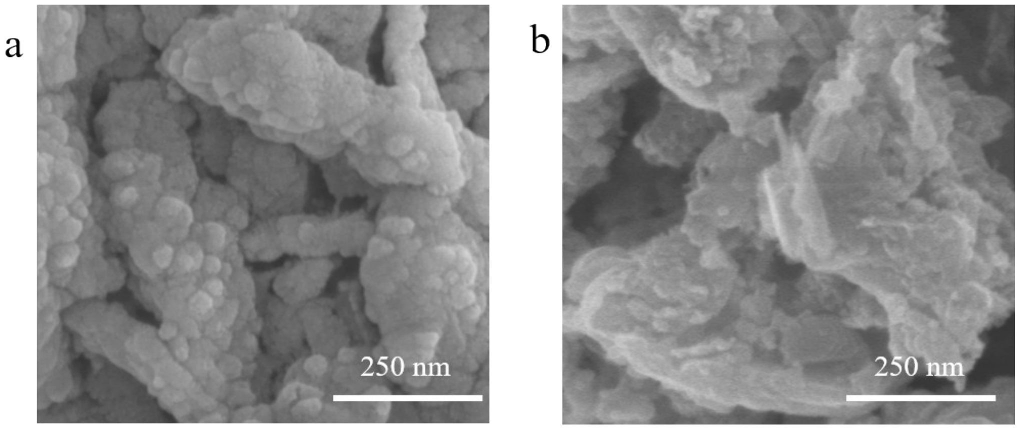

Fig. S9 SEM images of Co-Mo_2N@NC (a) before and (b) after 2000 cycles.

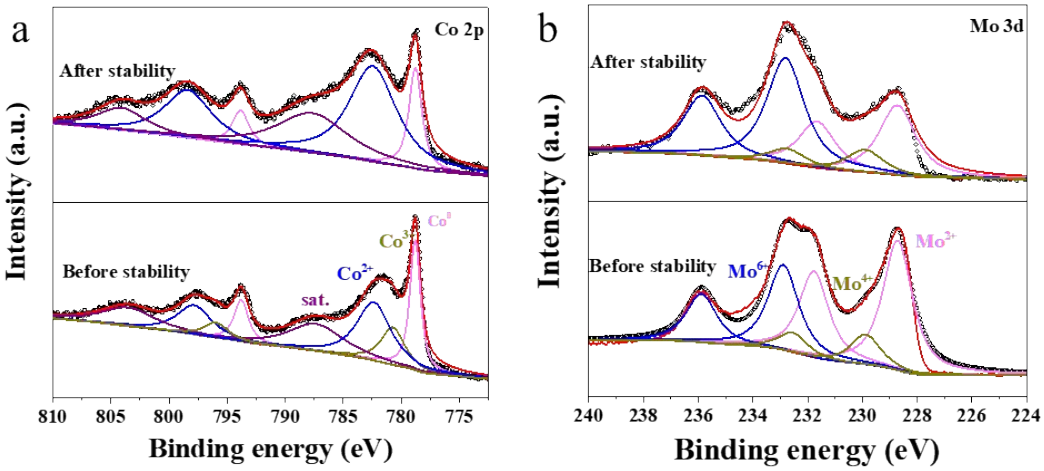

Fig. S10 XPS results of (a) Co 2p and (b) Mo 3d for Co-Mo_2N@NC before and after stability test for HER.

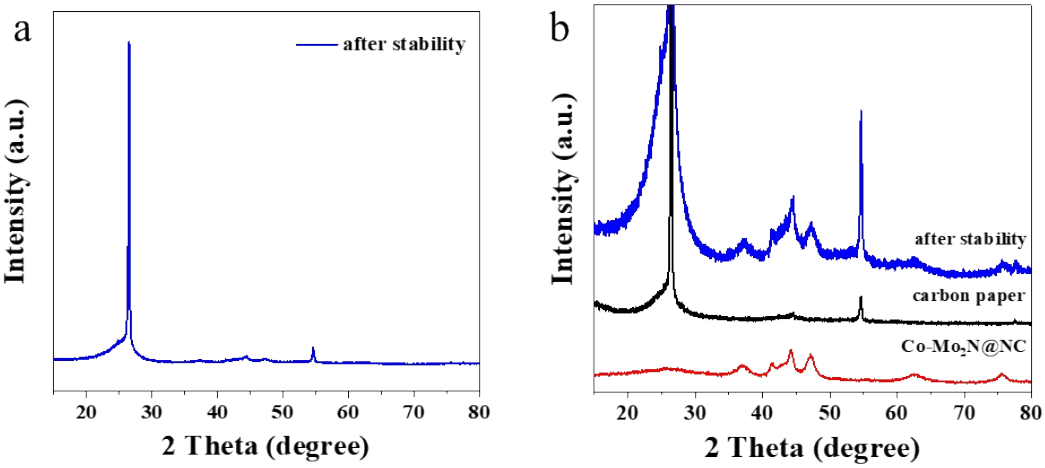

Fig. S11 (a) XRD result of Co-Mo_2N@NC loaded on carbon paper after stability test in HER. (b) enlarged XRD results of Co-Mo_2N@NC before and after stability test.

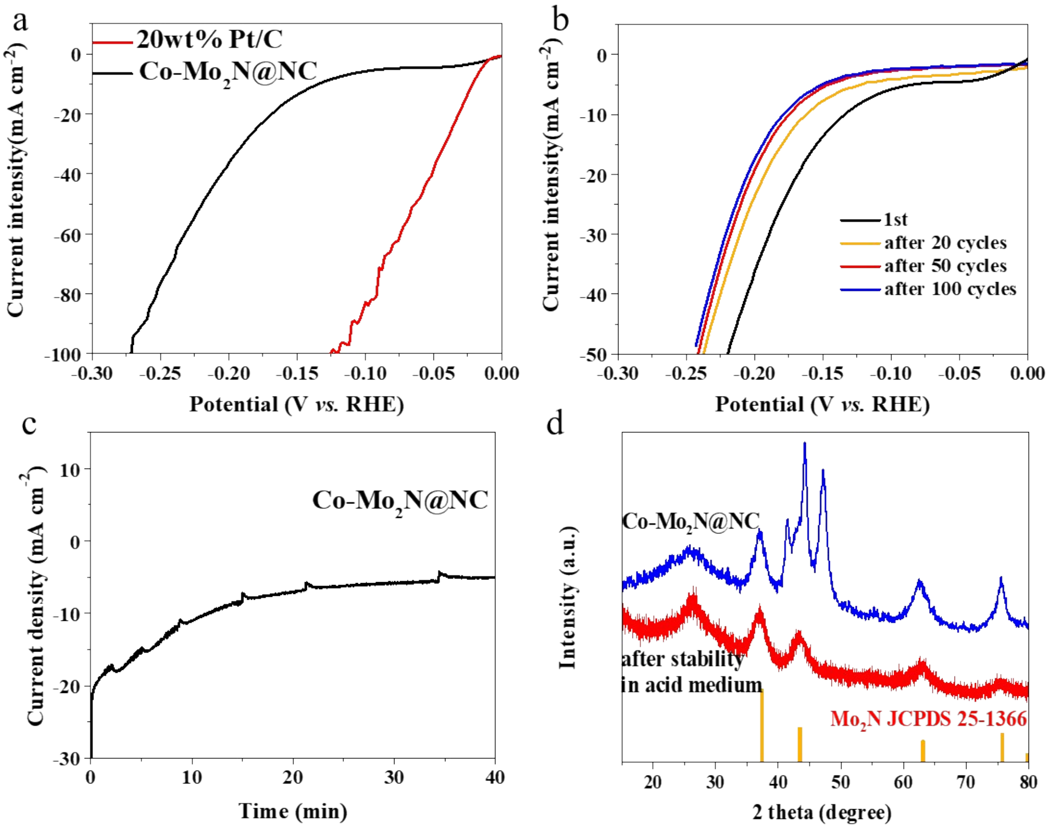

Fig. S12 (a) Polarization curves of Co-Mo_2N@NC in 0.5M H_2SO_4, (b) polarization curves before and after 20, 50 and 100 cycles, (c) time-dependent current density curve of Co-Mo_2N@NC under 160 mV and (d) XRD result of Co-Mo_2N@NC before and after stability test in acid medium.

Table S3. Summary of HER performance of different Mo-based and transition-metal-based catalysts for HER in 1 M KOH solution.

Materials	electrode	loading ($mg\cdot cm^{-2}$)	η_{onset} (mV *vs.* RHE)	η_{10} (mV *vs.* RHE)	Tafel slope (mV dec^{-1})	Ref
Co-Mo_2N@NC	glassy carbon	1.34	10	47	43	This work
Mo_2N@NC	glassy carbon	1.34	26	85	54	1
Mo_2C/NCF	glassy carbon	0.28	38	100	65	4
Mo_2C@C	glassy carbon	0.9	-	47	71	5
WN/Co	glassy carbon	1.12	17	76	98	6
Ni_3Fe@N-	glassy carbon	0.57	-	72	98	7
mNCMo_2C@rGO	glassy carbon	0.24	40	95	50	8
Co-Mo_2C	glassy carbon	0.14	25	118	44	9
$Co_2Mo_3O_8$/Co/NF	nickel foam	3.2	9	50	49	10
$NiCo_2O_4$	nickel foam	1.0	50	110	50	11
NC@$CuCo_2Nx$/C	carbon fiber	2.0	-	105	76	12
Co-MoS_2/BCCF	carbon paper	2.0	20	48	52	13
NiMoN-550	carbon paper	3.5	-	89	79	14
Co-MoS_2	carbon paper	2.0	30	90	50	15
Mo_2C	carbon fiber paper	-	-	96	99	16
N@Mo_2C	carbon fiber paper	2.0	-	66	49	17

Reference

1 Z. Lv, M. Tahir, X. Lang, G. Yuan, L. Pan, X. Zhang and J.-J. Zou, *J. Mater. Chem. A*, 2017, **5**, 20932-20937.

2 Y. Yao, N. Mahmood, L. Pan, G. Shen, R. Zhang, R. Gao, F. Aleem, X. Yuan, X. Zhang and J.-J. Zou, *Nanoscale*, 2018, **10**, 21327-21334.

3 X.-D. Wang, Y.-F. Xu, H.-S. Rao, W.-J. Xu, H.-Y. Chen, W.-X. Zhang, D.-B. Kuang and C.-Y. Su, *Energy Environ. Sci.*, 2016, **9**, 1468-1475.

4 Y. Huang, Q. Gong, X. Song, K. Feng, K. Nie, F. Zhao, Y. Wang, M. Zeng, J. Zhong and Y. Li, *ACS Nano*, 2016, **10**, 11337-11343.

5 Y.-Y. Chen, Y. Zhang, W.-J. Jiang, X. Zhang, Z. Dai, L.-J. Wan and J.-S. Hu, *ACS Nano*, 2016, **10**, 8851-8860.

6 H. Jin, H. Zhang, J. Chen, S. Mao, Z. Jiang and Y. Wang, *J. Mater. Chem. A*, 2018, **6**, 10967-10975.

7 T. Li, G. Luo, K. Liu, X. Li, D. Sun, L. Xu, Y. Li and Y. Tang, *Adv. Funct. Mater.,* 2018, **28**, 1805828.

8 D. Hou, S. Zhu, H. Tian, H. Wei, X. Feng and Y. Mai, *ACS Appl. Mater. Interfaces*, 2018, **10**, 40800-40807.

9 H. Lin, N. Liu, Z. Shi, Y. Guo, Y. Tang and Q. Gao, *Adv. Funct. Mater.*, 2016, **26**, 5590-5598.

10 Y. Ou, W. Tian, L. Liu, Y. Zhang and P. Xiao, *J. Mater. Chem. A*, 2018, **6**, 5217-5228.

11 X. Gao, H. Zhang, Q. Li, X. Yu, Z. Hong, X. Zhang, C. Liang and Z. Lin, *Angew. Chem. Int. Ed*, 2016, **55**, 6290-6294.

12 J. Zheng, X. Chen, X. Zhong, S. Li, T. Liu, G. Zhuang, X. Li, S. Deng, D. Mei and J.-G. Wang, *Adv. Funct. Mater.*, 2017, **27**, 1704169.

13 Q. Xiong, Y. Wang, P. F. Liu, L. R. Zheng, G. Wang, H. G. Yang, P. K. Wong, H. Zhang and H. Zhao, *Adv. Mater.*, 2018, **30**, 1801450.

14 Z. Yin, Y. Sun, C. Zhu, C. Li, X. Zhang and Y. Chen, *J. Mater. Chem. A*, 2017, **5**, 13648-13658.

15 Q. Xiong, X. Zhang, H. Wang, G. Liu, G. Wang, H. Zhang and H. Zhao, *Chem. Commun.*, 2018, **54**, 3859-3862.

16 W. Yuan, Q. Huang, X. Yang, Z. Cui, S. Zhu, Z. Li, S. Du, N. Qiu and Y. Liang, *ACS Appl. Mater. Interfaces*, 2018, **10**, 40500-40508.

17 Y. Huang, J. Hu, H. Xu, W. Bian, J. Ge, D. Zang, D. Cheng, Y. Lv, C. Zhang, J. Gu and Y. Wei, *Adv. Energy Mater.*, 2018, **8**, 1800789.